

# The Acceleration Scale, Modified Newtonian Dynamics, and Sterile Neutrinos

Antonaldo Diaferio and Garry W. Angus

**Abstract** General Relativity is able to describe the dynamics of galaxies and larger cosmic structures only if most of the matter in the Universe is dark, namely it does not emit any electromagnetic radiation. Intriguingly, on the scale of galaxies, there is strong observational evidence that the presence of dark matter appears to be necessary only when the gravitational field inferred from the distribution of the luminous matter falls below an acceleration of the order of  $10^{-10} \text{ m s}^{-2}$ . In the standard model, which combines Newtonian gravity with dark matter, the origin of this acceleration scale is challenging and remains unsolved. On the contrary, the full set of observations can be neatly described, and were partly predicted, by a modification of Newtonian dynamics, dubbed MOND, that does not resort to the existence of dark matter. On the scale of galaxy clusters and beyond, however, MOND is not as successful as on the scale of galaxies, and the existence of some dark matter appears unavoidable. A model combining MOND with hot dark matter made of sterile neutrinos seems to be able to describe most of the astrophysical phenomenology, from the power spectrum of the cosmic microwave background anisotropies to the dynamics of dwarf galaxies. Whether there exists a yet unknown covariant theory that contains General Relativity and Newtonian gravity in the weak field limit, and MOND as the ultra-weak field limit is still an open question.

---

Invited review contribution to *Gravity: Where Do We Stand?* edited by R. Peron, V. Gorini and U. Moschella, © Canopus Academic Publishing Limited, in press.

Antonaldo Diaferio

Dipartimento di Fisica, Università degli Studi di Torino, and Istituto Nazionale di Fisica Nucleare (INFN), Sezione di Torino, Via P. Giuria 1, 10125, Torino, Italy, e-mail: diaferio@ph.unito.it

Garry W. Angus

Astrophysics, Cosmology and Gravity Centre, University of Cape Town, Private Bag X3, Rondebosch, 7700, South Africa, e-mail: angus.gz@gmail.com

## 1 Introduction

The dynamical properties of galaxies and larger cosmic structures should be described by their mass content if gravity is the dominant force field. In 1932, Oort noticed a shortage of mass required to describe the velocity of stars in the solar neighbourhood [111]. In 1933, Zwicky found the very same problem by applying the virial theorem to the Coma cluster, based on the radial velocities of a few galaxies derived from their optical spectra [153]. These early discoveries were revived in the seventies when the existence of flat rotation curves in disk galaxies [120] and the requirement of the dynamical stability of galactic disks [112, 44] showed that a large fraction of mass, in addition to the observed luminous mass, was necessary to describe the dynamics of galaxies. Ever since, the evidence of missing mass in cosmic structures has become overwhelming [39].

General Relativity (GR) has encountered such a plethora of successes in the solar system that the scientific community finds it hard to suppose that GR, and its Newtonian weak field limit, might fail on cosmic scales. It is more natural to suppose that this missing mass is actually some form of dark matter (DM) that does not emit any electromagnetic radiation but only acts gravitationally.

This idea meets the demand of particle physics: going beyond the standard model of particle physics requires the existence of still unknown elementary particles, like, for example, supersymmetric particles, axions, Kaluza-Klein excitations, or sterile neutrinos. These particles may naturally play the role of the astrophysical DM [18]: they formed in the early Universe and their relic abundance can fill in the fraction of mass that is required to describe both the internal dynamics of structures and their formation by gravitational instability.

In addition, most of these particles have the advantage of being non-baryonic, namely, in the astrophysical jargon, they are neither electrons nor particles made of quarks. Non-baryonic matter includes neutrinos and the hypothetical Weakly Interacting Massive Particles (WIMPs). So far, only neutrinos have been detected; all other non-baryonic matter is still hypothetical.

Being non-baryonic is advantageous if gravitational instability drives the formation of the cosmic structure. In fact, in the inflationary scenario of the standard hot Big Bang cosmology, small perturbations due to quantum fluctuations are inflated to cosmic scales by the  $\sim 100$   $e$ -folding expansion of the Universe and provide the initial conditions of the matter density field. However, this scenario is contradicted by the Cosmic Microwave Background (CMB) anisotropies if the matter density field is mostly baryonic. In fact, the observation of temperature anisotropies  $\delta T/T = \delta/3$ , with  $\delta$  the baryonic matter density fluctuations, in the CMB, which formed by redshift  $z \sim 10^3$ , yields  $\delta T/T \sim 10^{-5}$  on  $\theta \sim 7^\circ$  angular scales, corresponding to superclusters and larger structures [135]. Gravitational instability yields a growth rate  $\propto (1+z)^{-1}$ , or slower. Thus, superclusters would have matter overdensities  $\delta$  of the order of  $\sim 10^{-2}$  today, rather than the observed  $\delta \sim 1 - 10$ . Non-baryonic DM decouples from the radiation field much earlier than baryons and its density perturbations can start growing at the time of equivalence, when the radiation and matter energy densities are equal. At the time of the baryon-radiation decoupling, DM per-

turbations have already grown to  $\delta \sim 10^{-2} - 10^{-3}$  on supercluster scales and they will keep growing to  $\delta \sim 1 - 10$  by today.

Further evidence of the non-baryonic nature of DM is the abundance of light elements which are synthesized in the early Universe. Measures of the primordial abundance of deuterium, for example, which is particularly sensitive to the photon-to-baryon ratio, implies a baryon density  $\Omega_b h^2 = 0.0214 \pm 0.0020^1$  [69], which agrees with the baryon density  $\Omega_b h^2 = 0.02229 \pm 0.00073$  implied by the CMB anisotropies [136], yet it is smaller than the total matter density  $\Omega_m h^2 = 0.114$  [71].

By combining all these pieces of evidence, the standard interpretation of the observations of the cosmic structure, from galactic scales to the CMB, suggests that only 17% of the matter in the Universe is baryonic, whereas the remaining 83% is required to be non-baryonic cold DM [71]. The entire amount of matter however yields only 27% of the matter-energy density required to make the Universe geometrically flat, as suggested by the CMB power spectrum [37]. The missing 73% can be easily described by a cosmological constant [19], but a large fraction of the cosmological community is searching for more sophisticated models, some of them including an additional dark energy (DE) fluid [39].

The current standard  $\Lambda$ CDM model thus contains non-baryonic cold DM and a cosmological constant  $\Lambda$ . However, we are in the uneasy situation where only 4.5% of the matter-energy density of the Universe is made of matter we can detect in laboratories on Earth. The rest is hypothetical (DM) and has unusual properties, like negative pressure ( $\Lambda$  or DE). To avoid this situation, the alternative solution is to assume that GR breaks down at some scale. A number of extended or modified theories of gravity have been suggested. Among them, Milgrom [94] proposed Modified Newtonian Dynamics (MOND), an empirical law that modifies Newtonian dynamics and actually goes beyond a simple alternative theory of gravity. MOND can elegantly deal with the galaxy scale phenomenology without DM but is less successful at describing the dynamical properties of galaxy clusters. Famaey and McGaugh [48] have recently extensively reviewed this model. Here, we summarize the successes of MOND and mention how the combination of MOND with the existence of sterile neutrinos of mass in the range 11 eV–1 keV can provide a reasonable description of the observed phenomenology, from galaxy scales to the CMB.

## 2 The Acceleration Scale

In 1983, MOND was originally introduced to explain the observed rotation curves of spiral galaxies [94]: the observed velocities of the stars are larger than the velocities that Newtonian dynamics would predict based on the distribution of the luminous matter [120]. As we mentioned above, this observational piece of evidence suggested the existence of some hidden mass, or DM, responsible for a stronger gravitational field and hence larger velocities. An alternative solution is that, on

---

<sup>1</sup> We use the standard parametrization for the Hubble constant today  $H_0 = 100 h \text{ km s}^{-1} \text{ Mpc}^{-1}$ .

these cosmic scales, Newtonian gravity does not hold. Milgrom [94] went beyond the suggestion of a modified theory of gravity that becomes relevant beyond some large length scale. He rather suggested that Newtonian dynamics breaks down below an acceleration scale  $a_0$ . In the formulation of classical physics, the relation between the acceleration  $\mathbf{a}$  acting on a point mass and the Newtonian acceleration  $\mathbf{a}_N$  is

$$\mu\left(\frac{|\mathbf{a}|}{a_0}\right)\mathbf{a} = \mathbf{a}_N, \quad (1)$$

where  $\mu(x)$  is an unknown interpolating function that satisfies the conditions  $\mu(x \rightarrow +\infty) = 1$  and  $\mu(x \rightarrow 0) = x$ .<sup>2</sup> To describe the observed rotation curves of spiral galaxies, we need to have the acceleration scale  $a_0 \approx 10^{-10} \text{ m s}^{-2}$  [95]. Moreover, Milgrom showed that this modification of Newtonian dynamics also drastically reduces the amount of DM required in groups and clusters of galaxies [96].

More importantly, Milgrom's suggestion provided clean predictions [95] that were confirmed in later years. Most notably: (1) the zero point of the Tully-Fisher relation; (2) the one-to-one correspondence between features in the baryonic distribution and the rotation curve; (3) a larger mass discrepancy, when interpreted with Newtonian gravity, in low surface brightness dwarf spheroidal galaxies; and (4) the validity of the Tully-Fisher relation for low surface brightness disk galaxies.

It also became clear very soon that there are different numerical coincidences that might suggest that  $a_0$  is indeed a fundamental quantity (see [17] for a recent review). For example, it is rather intriguing that  $a_0$  is related to the Hubble constant  $H_0$  and the cosmological constant  $\Lambda$  with the relations  $a_0 = cH_0/2\pi$  and  $a_0^2 = c^2\Lambda/2\pi$ , where  $c$  is the speed of light.

A compilation of kinematic and photometric data of disk galaxies very clearly shows the validity of this *ansatz* on the acceleration scale [87]: disk galaxies do not require DM beyond a given length scale, but rather below a given acceleration scale. Figure 1 shows the ratio between the observed velocity  $V$  and the velocity  $V_b$  expected in Newtonian gravity from the distribution of the visible matter. The square of this ratio is proportional to the ratio between the total mass and the visible mass in a spherical system. Evidently,  $(V/V_b)^2 > 1$  reflects a mass discrepancy and the requirement of DM; the larger the ratio the larger is the contribution of DM. Figure 1 clearly shows that the need for DM increases with decreasing Newtonian acceleration  $g_N = V_b^2/r$  which is proportional to the baryonic surface density. The MOND prediction is thus that low-surface brightness (LSB) galaxies are more DM domi-

<sup>2</sup> A year later, Bekenstein and Milgrom [15] showed that, in spherical symmetry, equation (1) is equivalent to a modified theory of gravity where the standard Poisson equation is replaced by

$$\nabla \cdot \left[ \mu\left(\frac{|\nabla\Phi|}{a_0}\right) \nabla\Phi \right] = 4\pi G\rho, \quad (2)$$

where  $\Phi$  is the gravitational potential and  $\rho$  the mass distribution. A more recent modified theory of gravity that reproduces equation (1) is the quasi-linear formulation of MOND (QUMOND) [103]. This theory has the advantage of involving only linear differential equations and one non-linear algebraic step. See [48] for a comprehensive review of the various formulations of MOND as modified dynamics or modified gravity.

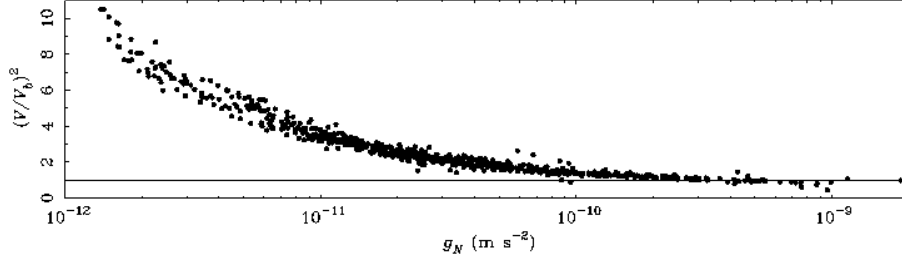


**Fig. 1**  $(V/V_b)^2$  vs. the Newtonian gravity  $g_N = V_b^2/r$ , derived from the baryonic surface density, in almost one hundred spiral galaxies. The need for DM appears when  $(V/V_b)^2 > 1$ . Observations clearly show that this only happens below a specific acceleration of the order of  $10^{-10} \text{ m s}^{-2}$ . Courtesy of B. Famaey and S. McGaugh. Reproduced from [48], with permission.

nated than high-surface brightness (HSB) galaxies in Newtonian gravity. However, the Tully-Fisher relation, that we describe below, remains valid for both classes of galaxies. In the DM paradigm, it is unclear how the tight correlation shown in Figure 1 can emerge from the combination of intrinsically chaotic processes, including the history of the DM halo formation, the star formation history and feedback processes.

If this acceleration scale does indeed exist, we have two relevant consequences: (1) MOND has to break the Strong Equivalence Principle, which states that all laws of physics are independent of velocity and location in spacetime, and (2) Birkhoff's theorem is not valid.

MOND is not required to break the Weak Equivalence Principle which asserts the equality between inertial and gravitational masses. In GR, the Weak Equivalence Principle translates into the assumption that all matter fields are coupled to the geodesic metric  $g_{\mu\nu}$ , whereas the Strong Equivalence Principle is guaranteed by assuming that the same metric  $g_{\mu\nu}$  obeys the Einstein-Hilbert action  $S_{\text{EH}} = c^4/(16\pi G) \int g^{\mu\nu} R_{\mu\nu} (-g)^{1/2} d^4x$ , where  $R_{\mu\nu}$  is the Ricci tensor and  $g$  the determinant of the metric. Therefore, one way to break the Strong Equivalence Principle is to keep the Einstein and geodesic metrics distinct.

The non-validity of Birkhoff's theorem clearly complicates the interpretation of the dynamical properties of self-gravitating systems. In Newtonian gravity, any object is subject to the gravitational attraction of all the other objects in the Universe, but in Newtonian linear dynamics a star in a galaxy or a galaxy in a galaxy cluster are virtually isolated from the gravitational field felt by the parent system, unless this latter external field varies across the parent system and originates the well known effect of tides. In MOND, the external field affects the internal motions of the objects even when this field is constant, because it is the total acceleration felt by the object that determines the dynamical, MONDian or Newtonian, regime. We will mention below that this issue can be relevant in the investigation of the internal dynamics of elliptical galaxies, that are mostly located in regions of high galaxy density, and dwarf spheroidal galaxies and globular clusters, that are satellites of larger galaxies.

In Sect. 4, we describe an example of how these issues enter the construction of a covariant theory of MOND.

### 3 Self-gravitating Systems

#### 3.1 Disk Galaxies

On the scales of galaxies there are a number of observations that were either predicted or easily explained by MOND. In the DM paradigm, these very same observations require extreme fine tuning between baryonic and non-baryonic physics or even yet undiscovered mechanisms.

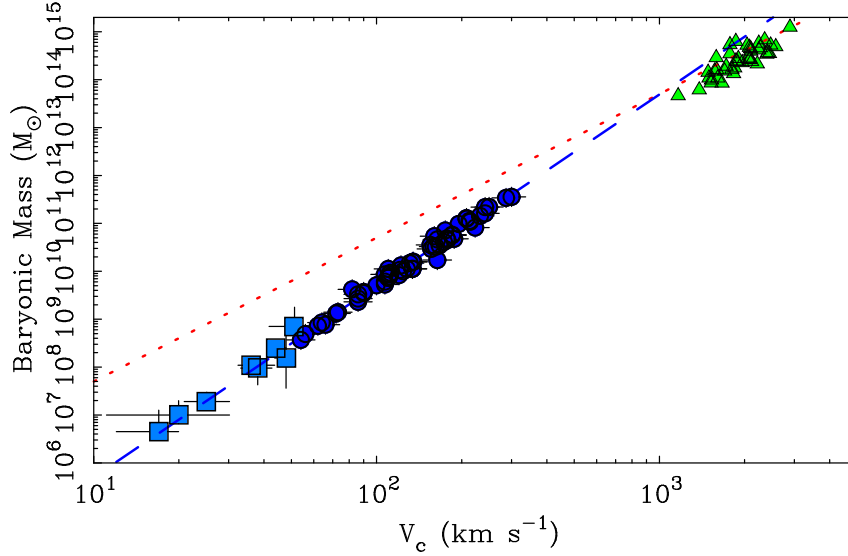


**Fig. 2** Baryonic mass  $M_b$  vs. circular velocity  $V_c$  in dwarf (squares) and spiral (circles) galaxies [89] and in clusters of galaxies (triangles; [119]). The blue dashed line is the fit to the spiral galaxies alone  $M_b = 50(V_c/\text{km s}^{-1})^4 M_\odot$ . The red dotted line is the simplest standard model expectation if all the baryons in each DM halo are identified. Courtesy of S. McGaugh. Reproduced from [90], with permission.

Tully and Fisher [145] showed that, in disk galaxies, the maximum rotation velocity  $v_{\text{rot}}$  is proportional to the galaxy luminosity. MOND predicts that at large radii  $a^2/a_0 \sim a_N = GM_b/r^2$  (equation 1) and from  $a = v_{\text{rot}}^2/r$  we obtain

$$v_{\text{rot}}^4 = GM_b a_0, \quad (3)$$

where  $M_b$  is the baryonic mass. Figure 2 shows the measured baryonic mass  $M_b$  as a function of the measured circular velocity  $V_c$  for astrophysical systems on different scales, from dwarf galaxies (left bottom corner) to clusters of galaxies (upper right corner).  $V_c$  is a characteristic circular velocity measured in the outer region of the system [90]. The blue dashed line shows the relation  $M_b = 50(V_c/\text{km s}^{-1})^4 M_\odot$ . The MOND prediction clearly agrees with both the observed slope and normalization. In addition, the observed spread is consistent with the uncertainties. This result implies that the relation  $v_{\text{rot}}^4 = GM_b a_0$  holds exactly.

In the standard model, disk galaxies are embedded in DM halos whose average density within their virial radius is basically independent of the halo mass. It is thus usual to define  $r_{200}$  as the radius within which the average density is 200 times the critical density of the Universe. It follows that for  $M_{200}$ , the mass within  $r_{200}$ , we have  $M_{200} \propto r_{200}^3$  and the circular velocity  $V_c = (GM_{200}/r_{200})^{1/2} \propto M_{200}^{1/3}$ . This relation is shown as the red dotted line in Figure 2. The circular velocity is not necessarily identical to the disk rotation velocity  $v_{\text{rot}}$ , because of the complex interplay between the merger history of the DM halo and the star formation history and energy feedback of the galaxy. For example, we could easily recover the correct slope  $v_{\text{rot}}^4 \propto M_b$ , by assuming that luminosity traces the total mass ( $L \propto M_b \propto M_{\text{tot}}$ ) and that the density and scale height of the galaxy disk is roughly constant in disk galaxies; this latter assumption implies  $M_{\text{tot}} \propto R^2$  where  $R$  is the disk size. From  $v_{\text{rot}}^2 = GM_{\text{tot}}/R$ , we correctly derive  $v_{\text{rot}}^4 \propto M_b$ . A rigorous comparison between observations and the standard model is not trivial [137], but recent analyses, where properly balanced contributions of the various physical and observational effects are carefully blended, seem to bring the  $\Lambda$ CDM Tully-Fisher relation in better agreement with observations [38, 42].

However, in the standard model, the predicted scatter remains larger than observed, because, unlike MOND, we do expect that the galaxy merger and star formation history mentioned above introduce an intrinsic scatter. In addition, *a priori*, we do not have any reason to expect that (1) the observed relation extends over five orders of magnitude in baryonic mass, from dwarf galaxies to massive disk galaxies, again with basically no scatter, as shown in Figure 2; and that (2) the LSB galaxies, that should presumably have a star formation efficiency lower than normal galaxies [150, 146], also perfectly fit into this relation. This latter result was originally predicted by Milgrom [95], fifteen years before the measurements of the rotation curves of LSB galaxies [92].

MOND goes beyond the description of global properties of disk galaxies. Figure 3 shows the observed rotation curves of a HSB galaxy and a LSB galaxy (open symbols with error bars). The rotation curves expected in Newtonian gravity from the distribution of baryonic matter (black solid lines) severely underestimate the observations. The underestimate increases with distance  $R$  from the galaxy center and is larger for the LSB galaxy. In the standard model, this observation is explained by increasing the DM contribution with increasing  $R$  and decreasing galaxy luminosity. This solution is usually motivated by a lower star formation efficiencies at larger radii, as suggested by extensive surveys of neutral hydrogen in nearby galaxies [81, 21].

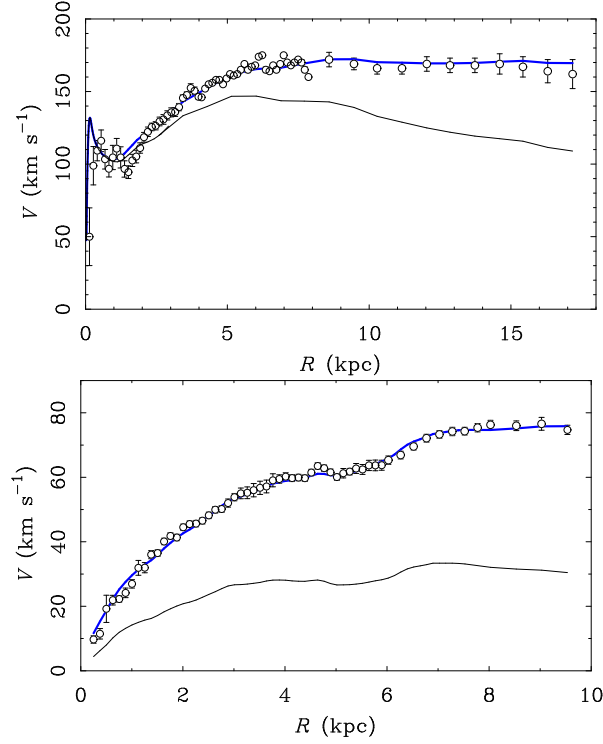


**Fig. 3** Examples of MOND rotation curve fits of a HSB galaxy (NGC 6946, top panel) and a LSB galaxy (NGC 1560, bottom panel). The black lines show the Newtonian rotation curve expected from the observed distribution of stars and gas. The blue lines are the MOND fits with best fit stellar mass-to-light ratios in the  $K$ -band  $0.37 M_{\odot}/L_{\odot}$  (NGC 6946) and  $0.18 M_{\odot}/L_{\odot}$  (NGC 1560). Courtesy of B. Famaey and S. McGaugh. Reproduced from [48], with permission.

What is more remarkable is that the small scale features of the rotation curves mirror the distribution of the baryonic matter in the disk. This characteristic is shared by the rotation curves expected in Newtonian gravity from the distribution of baryonic matter (black solid lines in Figure 3). In the standard model, this property of the total rotation curve is unexpected, because this rotation curve should be mostly determined by the dynamically dominant DM distribution and the baryonic distribution should play a very minor role. On the contrary, MOND describes the observations with impressive accuracy (blue solid lines), including the small scale features of the curves.

The MOND curves are derived with a single free parameter, the stellar mass-to-light ratio of the disk, in addition to the distance to the galaxy required to determine its length and hence acceleration scales; the best fit values of the mass-to-light ratios are in perfect agreement with values derived from stellar population synthesis models. Moreover, redder galaxies require larger mass-to-light ratios, as expected on completely independent astrophysical grounds [16]. This limited freedom of MOND



should be compared with the standard model that requires two parameters for the DM halo of each galaxy and a global mass-to-light ratio of the galaxy that depends on  $R$  and is unrelated to the mass-to-light ratios of the stellar populations.

The agreement shown in Figure 3 is common to 75 nearby galaxies to date [48]. Among these, an interesting case is NGC 7814: this galaxy is almost perfectly edge-on and the uncertainties on the rotation curve deriving from the disk inclination are negligible; in addition, the distance to the galaxy is accurate to 5% and is basically not a free parameter any longer. This galaxy provides a stringent test for MOND: high-quality infrared photometric observations [54] enable, for the first time, the construction, from an accurate bulge-disk decomposition, of a three-dimensional model of the galaxy whose gravitational potential is inferred by numerically solving the MONDian Poisson equation. The comparison of the model rotation curve with the observed one allows the derivation of the mass-to-light ratios for both the disk and the bulge components. Both ratios are found to be in excellent agreement with the expected values [10].

The data expected in the upcoming GAIA mission and other future surveys will provide unprecedented possibilities to test MOND with the Milky Way dynamics [48]. Pioneering work with current data has already shown that the rotation curve and the surface density of the inner disk of the Milky Way are fully consistent with each other within the MOND framework [91, 47]. Similarly, the escape velocity from the solar neighbourhood agrees with current estimates if the external gravitational field in which the Milky Way is embedded is  $a \sim 10^{-2}a_0$ : this value is indeed compatible with the actual field [46]. An additional test involves the velocity ellipsoid tilt angle within the meridional galactic plane. The angles expected in MOND and in the standard Newtonian gravity with DM agree with each other and with observations at galactic heights  $z = 1$  kpc; however, the discrepancy between the predicted angles in the two models increases with  $z$  and the measure of the velocity ellipsoid tilt angle will thus be a relevant test to discriminate between the models [20].

### 3.2 Elliptical Galaxies

The role played by the acceleration scale is also evident in elliptical galaxies, dwarf spheroidal galaxies (dSphs) and globular clusters.

In elliptical galaxies, that are pressure supported systems, Faber and Jackson [45] observed a relation similar to the Tully-Fisher relation that is valid for disk galaxies: the galaxy luminosity  $L$  correlates with the stellar velocity dispersion  $\sigma$  in the galaxy's central region, according to the power law  $L \propto \sigma^4$ . If we assume that ellipticals are isothermal spheres that, in MOND, have finite mass with asymptotically decreasing density  $\rho \propto r^\alpha$ , with  $\alpha = d \ln \rho / d \ln r = -4$ , we find  $\sigma^4 = GM_b a_0 / \alpha^2$  [97]. Unlike the Tully-Fisher relation, the observed Faber-Jackson relation is not expected to be exact in MOND, because ellipticals are not strictly isothermal and their velocity field is not isotropic; the velocity anisotropy parameter must actually

vary with radius to match the observed Fundamental Plane of ellipticals [124]. The MOND Fundamental Plane is actually slightly tilted compared to observations, but this problem might be removed by including the external field effect [28].

Elliptical galaxies pose some challenges to the standard model, because they should be embedded, like disk galaxies, in DM halos. X-ray emitting hot gas coronae are expected signatures of a DM halo and are indeed observed in many early type galaxies [113], including isolated ellipticals, like NGC1521 [65]. However, there are cases that are unexpected in the DM paradigm: accurate observations, based on planetary nebulae, of the kinematics of the outer parts of three ordinary ellipticals show very little evidence, if any, of the presence of DM [121], but are in good agreement with MOND, because the large masses implied by the high surface brightnesses indicate that the gravitational field is in the Newtonian regime  $a > a_0$  [105, 142].

The kinematics of the outskirts of ellipticals, where  $a < a_0$ , can be probed with spectroscopic observations of their globular cluster systems: for example the galaxy NGC4636 in the Virgo cluster is surrounded by 460 globular clusters with measured velocity and this sample represents one of the largest currently available. The MONDian predictions agree with the kinematic data and NGC4636 also appears to fall onto the baryonic Tully-Fisher relation shown in Figure 2 [128].

The X-ray data available for NGC1521 and NGC720 offer a unique test of MOND in elliptical galaxies: these galaxies are not embedded in groups or clusters and the X-ray data extend to large radii. Similarly to disk galaxies, one can thus test MOND in the outskirts of galaxies where the gravitational acceleration due to the luminous matter is smaller than  $a_0$  and the external field effect is negligible. MOND describes the distribution of the baryonic mass in these galaxies with mass-to-light ratios fully consistent with stellar population synthesis models [104].

### 3.3 Dwarf Spheroidals

At the low mass end of the galaxy mass function, dSphs also pose a challenge to the standard model (see [72] for a recent review of dSphs in MOND). dSphs have low surface brightnesses and, according to MOND, based on what is shown in Figure 1 for disk galaxies, Milgrom predicted that they should be DM dominated and have mass discrepancies larger than ten when analyzed with Newtonian gravity [95]. This prediction was impressively confirmed when the first measures of the stellar velocity dispersion in the central regions of these galaxies were available a decade later [98].

More recently, intense observational programs provided velocity dispersion profiles of the dSphs orbiting the Milky Way [149]. This piece of information enables the estimate of the combination of the mass profiles of the galaxies with the profiles of their velocity anisotropy parameter. The most recent detailed dynamical analysis [129] confirms that the mass-to-light ratios in the  $V$  band are in the range  $1 - 3 M_\odot/L_\odot$ , and are therefore consistent with stellar population synthesis models. This analysis solved an open issue raised earlier [2]: unbound stars can contaminate

the velocity dispersion and artificially inflate the estimate of the mass-to-light ratio. When the unbound stars are properly removed with the caustic technique [40, 130], Sculptor and Sextans do indeed show the sensible mass-to-light ratios  $1.8 M_{\odot}/L_{\odot}$  and  $2.7 M_{\odot}/L_{\odot}$  respectively, whereas Carina still shows a too large  $\sim 6 M_{\odot}/L_{\odot}$ .

This discrepancy might originate from (1) the uncertainties of the luminosity distribution that is challenging to estimate accurately enough in LSB galaxies, and (2) the ellipticity of Carina that significantly departs from the spherical symmetry assumed to derive the mass-to-light ratio. However, this discrepant mass-to-light ratio might have a deeper origin due to the specific feature of MOND that we mentioned in Sect. 2, the external gravitational field effect: a star in a dSph, that is a satellite of the Milky Way, moves according to both the dSph mass and the gravitational field exerted by the Milky Way; only if this latter external acceleration is negligible compared to the acceleration internal to the dSph is the dSph mass derived from the stellar velocity dispersion accurate. Carina is one of the least luminous, and presumably least massive, dSphs and one of the closest to the Milky Way. It is therefore reasonable to suspect that the Milky Way's gravitational field can play a role in inflating the velocity dispersion of this dSph. Although this suggestion still awaits a quantitative confirmation, this same effect appears to be responsible for the deviation of some dSphs from the expected Tully-Fisher relation shown in Figure 2 [93].

An additional piece of evidence, which is problematic for the standard model, is the phase-space distribution of the dSphs that are satellites of the Milky Way. These dSphs are distributed over an extended thin disk whose thickness is between 10 and 30 kpc and radius  $\sim 200$  kpc. An invoked solution is that these dSphs fell into the MW halo as a small group of galaxies who kept their orbits correlated [82]. However, recent measures of the dSph proper motions indicate that this scenario is untenable because, according to these measures, four dSphs must have fallen in at least 5 Gyr ago [12] and  $N$ -body simulations of the standard model show that the orbit correlation cannot be preserved for such a long time [70].

In MOND, dSphs may form as tidal debris during close encounters of large galaxies [76] and the orbit correlation would thus be a natural consequence of this formation process [114, 115]. The formation of tidal dwarf galaxies has been observed in interacting galaxies for the last twenty years [41], since the first detection in the Antennae [106]. The observed stellar velocities of these systems agree with MOND in the majority of the systems using sensible values of the two available free, but constrained, parameters, the mass-to-light ratio and the velocity anisotropy parameter  $\beta$  [101, 56]. In the standard model these systems are somewhat challenging because, in this case, the observed velocities require a factor of a few more mass than the observed luminous mass, despite the fact that there is no physical reason for these low surface brightness tidal dwarfs to drag large amounts of DM [22].

The formation of dwarf galaxies as tidal debris is also likely to solve the missing satellite problem of the standard model that predicts a factor of ten more satellites in the halos of large galaxies than is actually observed [107]. In MOND, the rate of galaxy encounters is small enough that it might provide the right number of satellites with the correct dynamics. On the contrary, in the standard model, a conspiracy

of processes regulating the star formation efficiency is required so that most DM satellites form no stars [62]. In addition, the possible supersonic relative velocity between baryons and DM before reionization might be responsible for the inhibition of the formation of half the expected luminous satellites [23]. If we take into account the ultra-faint galaxies surrounding the Milky Way, the problem can also be partly alleviated, but there would still be a factor of four too few dwarfs [134]. In addition these ultra-faint galaxies show indications of tidal disruption, although one would expect that, with mass-to-light ratios of the order of  $1000 M_{\odot}/L_{\odot}$ , the large DM halo within which they are embedded should be sufficient to screen the stellar components from the external tidal field of the Milky Way. The properties of dwarf galaxies thus remain challenging for the DM paradigm [25, 64, 75].

### 3.4 Globular Clusters

The good agreement between the expected dSph dynamics in MOND and observations is more intriguing when we consider globular clusters. These stellar systems and dSphs roughly have the same baryonic mass but different surface brightnesses, stellar populations and ages. In the standard model, globular clusters are devoid of DM, whereas dSphs are the cosmic structure with the largest fraction of DM, with mass-to-light ratios in the range  $\sim 10 - 1000 M_{\odot}/L_{\odot}$  [149, 148]. These discrepancies between globular clusters and dSphs are solved by invoking low formation efficiencies in low mass DM halos [74, 73] and two completely different formation processes for the two kinds of systems. On the contrary, in MOND, the different observed internal velocities is exactly what we expect from the different surface brightnesses (Figure 1) [55].

Nevertheless there is a system that requires careful consideration. NGC 2419 is a globular cluster in the outer halo of the Milky Way with low enough surface brightness to be in the MOND regime. It is far enough from the gravitational field of the Galaxy that the MOND external field effect might not play a relevant role. Similarly to the analyses of the dSphs, it is possible to estimate the mass-to-light ratio of the cluster from measurements of the projected velocity dispersion of the stars [66]. In MOND, the mass-to-light ratio required to describe the stellar kinematics is a factor of a few lower than expected (the opposite case as for the Carina dSph). Invoking a variable velocity anisotropy does not help improve the comparison between the MOND fit and the data, but non-isothermal polytropic models seem to provide a MONDian description of the kinematic and photometric observations of this cluster [126, 127]. An additional solution is that the life time of the globular cluster is long enough that mass segregation has already taken place. In this case, the distribution of RGB and luminous upper main sequence stars used in the Jeans analysis is expected to be more centrally concentrated than the other less massive stars of the clusters; therefore the true gravitational potential of the cluster might be different from the gravitational potential actually derived with the Jeans equation. Another

possibility is that globulars have non-standard initial stellar mass functions. More data and more testable globular clusters are clearly called for.

Another system that has seemed to be challenging for MOND is the five globular clusters orbiting the Fornax dSph. Fornax is the most luminous dwarf spheroidal (by about a factor of ten) and is the only classical dwarf of the Milky Way with a system of globulars. It was suggested that the surprisingly stronger dynamical friction due to the dwarf galaxy's low density component of stars in MOND, relative to the dynamical friction from the more dense DM halo in Newtonian gravity [34], would cause the globular clusters to lose their orbital angular momentum in a period of time much shorter than the Hubble time and create a stellar nucleus in Fornax which is not observed [122, 36]. However, Angus and Diaferio [4] used an orbit integrator with accurate mass models of Fornax both in MOND and Newtonian dynamics to convincingly demonstrate that the situation is relatively easy to explain: the globular clusters can orbit for a Hubble time as long as their orbits start near the tidal radius. This solution does not apply to the most massive globular cluster; however, this globular cluster is a statistic of one and could have a sizeable line of sight distance where the dynamical friction is negligible.

### 3.5 Groups and Clusters of Galaxies

The impressive agreement between observations and MOND predictions on the scale of galaxies, based on the introduction of the acceleration scale  $a_0$ , is not shared by the galaxy cluster data [139, 57]. Clusters do not perfectly obey the relation between circular velocity and baryonic mass of equation (3) (green triangles in Figure 2) but seem to require more mass than actually observed. In fact, in the core of clusters  $a > a_0$  and the luminous matter should be enough to describe the observed dynamics. The evidence suggests the opposite is true, because the amount of observed mass is a factor of two too small. The shortage of mass, which is confined to the central regions of clusters and progressively disappears in the cluster outskirts [7], is not as large as the factor of five or larger we have in the standard model, but it clearly poses a challenge to MOND.

An equivalent, more conventional way to look at Figure 2 for clusters is to consider the relation between the cluster mass and the X-ray temperature of the hot intracluster gas. According to the relation between mass and circular velocity, MOND makes a clear prediction for the mass-temperature relation. By assuming the same argument used for the Faber-Jackson relation in elliptical galaxies, the relation between the velocity dispersion  $\sigma$  of the galaxies in a cluster and the baryonic mass  $M_b$  of the cluster is  $\sigma^4 = GM_b a_0 / \alpha^2$ , where  $\alpha$  is the logarithmic slope of the mass density profile. The temperature  $T$  of the intracluster medium is a measure of the kinetic energy of the galaxies and  $T \propto \sigma^2$ . Therefore, in MOND, we have  $M_b \propto T^2$ . Figure 4 shows that the data agree with this scaling relation but not with the normalization, because of the mass discrepancy in the cluster cores mentioned above.

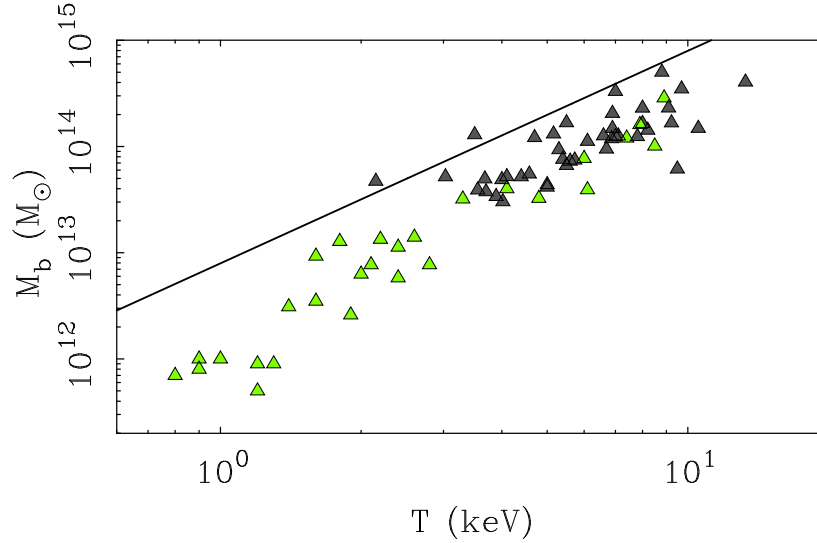


**Fig. 4** The baryonic mass–X-ray temperature relation for rich clusters (gray triangles [125]) and groups of galaxies (green triangles [7]). The solid line is the MOND prediction  $M_b \propto T^2$ . Courtesy of B. Famaey and S. McGaugh. Reproduced from [48], with permission.

This relation is not at odds with the standard model relation  $M \propto T^{3/2}$ ,<sup>3</sup> which is known to agree with observations [147], for two reasons. First, the  $M \propto T^{3/2}$  relation is between the X-ray temperature and the total cluster mass, which includes DM, rather than the baryonic mass alone that we have in the MOND  $M_b \propto T^2$  relation. Second, the mass  $M$  is inferred by assuming valid Newtonian gravity whereas  $M_b$  shown in Figure 4 is derived with MOND [7]. Nevertheless, we can neglect the latter reason and still see that the two scaling relations are roughly consistent with each other. In fact, in the standard model, we can write  $M = M_b / f_b \propto T^{3/2}$ , where  $f_b$  is the baryon fraction of the cluster total mass. Therefore, the observed MONDian  $M_b \propto T^2$  should imply  $f_b \propto T^{1/2}$ . This expectation is broadly consistent with observations: by combining X-ray Chandra groups and HIFLUGCS [151] over the temperature range [0.6, 15] keV, Eckmiller et al. [43] find  $f_b \sim T^{0.79 \pm 0.09}$  at  $r_{500}$ ; by limiting the sample to clusters with  $T$  in the range [1, 15] keV, the slope is  $0.83 \pm 0.42$ , but it appears to be shallower at smaller radii.

<sup>3</sup> In the standard model, the cluster virial mass scales as  $M_{\text{vir}} \propto \rho_c(z) \Delta_c(z) R^3$ , where  $R$  is the cluster size in proper units (not comoving),  $\rho_c(z) = 3H^2(z)/(8\pi G)$  is the critical density of the Universe, and  $\Delta_c(z)$  is the cluster density in units of  $\rho_c(z)$ . A widely used approximation is

$$\Delta_c(z) = 18\pi^2 + \begin{cases} 60w - 32w^2, & \Omega_m \leq 1, \quad \Omega_\Lambda = 0 \\ 82w - 39w^2, & \Omega_m + \Omega_\Lambda = 1 \end{cases} \quad (4)$$

where  $w = \Omega_m(z) - 1$  [27]. Now,  $\rho_c(z)$  scales with redshift  $z$  as  $\rho_c(z) \propto E^2(z) = \Omega_m(1+z)^3 + (1 - \Omega_m - \Omega_\Lambda)(1+z)^2 + \Omega_\Lambda$ . The cluster size thus scales as  $R \propto M_{\text{vir}}^{1/3} \Delta_c^{-1/3}(z) E^{-2/3}(z)$ , and the temperature as  $T \propto M_{\text{vir}}/R \propto M_{\text{vir}}^{2/3} \Delta_c^{1/3}(z) E^{2/3}(z)$ .

The apparent mass discrepancy in X-ray bright groups and clusters in MOND [7], clearly shown by the difference between the observed and predicted normalizations of the mass-temperature relation shown in Figure 4, does not seem to appear in groups of galaxies where the X-ray emission is negligible or absent [99, 100]. This piece of evidence might suggest that the mass discrepancy in MOND can be solved by assuming the presence of undetected baryonic mass in the form of cold, dense gas clouds that can form and be stable because of the presence of the ionised hot gas [102].

A different solution is that we might well have some DM that clusters on cluster scales but not on galaxy scale. The piece of evidence that is usually claimed to be difficult to interpret without assuming the existence of some form of DM comes from colliding galaxy clusters. During the collision of two clusters, the galaxies and the two halos of DM, if DM exists and is collisionless, keep their momentum, whereas the intracluster medium is shock heated and slows down. The DM and galaxy components thus separate from the gas component. This separation is clearly visible by combining X-ray and optical images of individual colliding clusters: for example, the so-called Bullet cluster 1E 0657-558 [35], and the cluster MACS J0024.4-1222 [26].

In the absence of DM, most of the matter resides in the gas rather than in the galaxies. The only way to measure how the total mass is distributed, is to derive a map of the gravitational potential with weak gravitational lensing. In GR, this procedure is now standard and in the two systems mentioned above, the mass appears to be concentrated where the galaxies are and not where the gas is: this is in striking agreement with the presence of some form of collisionless DM dominating the mass content of the cluster.

Unfortunately, a similar gravitational lensing analysis is not trivial in alternative theories of gravity where the effect of gravity on the light path is not treated properly. MOND belongs to this group of theories because it is a classical theory and gravitational lensing can only be described by resorting to one of the different covariant extensions of MOND. We will describe the results of this approach in Sect. 4. Here, we wish to emphasize that the location of the gravitational peaks is not an observational fact, but derives from the assumption of GR's validity. *A priori* it is possible that the non-linearity of a gravity theory alternative to GR is sufficient to mimic the observed gravitational lensing distortion with a mass distribution different from that required by GR. For example, in the covariant MOND theory named TeVeS, particular matter distributions can yield non-zero convergence on sky positions where there is no projected mass [9]. Weyl gravity provides another clear non-MONDian example of this phenomenology [116, 117].

There is a final cautionary comment that cannot be omitted: the interpretation of the observed properties of colliding clusters is far from being clear, because these systems can also be challenging for the standard model. The Abell cluster A520 has the same morphology of the Bullet cluster and MACS J0024.4-1222: two clouds of galaxies on the opposite sides of a cloud of hot gas [84, 67]. However, the GR weak lensing analysis indicates that, in addition to the two gravitational potential peaks at the location of the galaxies, there is a significant peak where the gas is. This



peak is difficult to explain in the standard model, because it requires the existence of a massive DM halo devoid of galaxies, but associated with the cluster hot gas. A number of possible solutions have been suggested, but none of them appears to be fully convincing [67].

In addition, colliding clusters appear to have relative velocities that are unlikely in the standard model: a system like the Bullet cluster, with a relative velocity derived from the shockwave of  $\sim 4700 \text{ km s}^{-1}$  [35], requires an initial infall velocity of the two clusters of  $\sim 3000 \text{ km s}^{-1}$  [85] that has a probability smaller than  $3.6 \times 10^{-9}$  to occur in  $\Lambda\text{CDM}$  [80]. On the contrary, the enhanced intensity of MOND gravity may naturally produce these large relative velocities [6, 5]. Similarly, the coherent motion of galaxy clusters on large scales, measured with a technique based on the kinematic Sunyaev-Zeldovich effect produced by Compton scattering of the CMB photons, appears to be challenging for the standard gravitational instability paradigm: these bulk flows are a factor of five larger than predicted by the standard model and might require a modification of the theory of gravity, among other possible solutions [68].

## 4 TeVeS and Gravitational Lensing

MOND, as described in Sect. 2, is a classical empirical law that we would like to recover as the weak field limit of a covariant theory. This theory should contain GR, that excellently describes the gravitational phenomenology of the solar system. A covariant theory for MOND is required if we wish to build a cosmological model and describe the gravitational lensing phenomenology within the MONDian framework. A covariant theory is thus essential for the validation of MOND.

The attempts to build a covariant theory containing MOND are numerous. A recent overview of these attempts is provided by Famaey and McGaugh [48]. Here, we briefly outline one of them, namely TeVeS (see [14] for a recent review), whose Lagrangian contains a time-like vector field and a scalar field in addition to the tensor field representing the metric, hence the name Te(nsor)Ve(ctor)S(calar). Halle et al. [63] have shown that a very general Lagrangian for a decaying vector field unifies most of the popular gravity theories, including quintessence,  $f(R)$ , Einstein-Aether theories, and TeVeS itself, among others. We stress that TeVeS by no means is the only possible covariant theory that yields MOND in the weak field limit. Moreover, it is clear that any problem or failure belonging to one of these covariant theories are not necessarily problems or failures of MOND.

TeVeS was first proposed by Bekenstein [13]. At the classical level, MOND introduces an acceleration scale. This issue poses an immediate problem for building a generally covariant theory, because the acceleration scale is played by the affine connection  $\Gamma_{\mu\nu}^{\kappa}$ , that involves the first derivatives of the metric tensor  $g_{\mu\nu}$ , and  $\Gamma_{\mu\nu}^{\kappa}$  is not a tensor. As we mentioned in Sect. 2, one way to bypass this problem is to distinguish between the Einstein metric  $g_{\mu\nu}$ , that enters the Einstein-Hilbert action, and the geodesic metric  $\tilde{g}_{\mu\nu}$ , that enters the matter action. In GR, the two metrics



coincide. In TeVeS, the two metrics are related by the equation<sup>4</sup> [123]

$$\tilde{g}_{\mu\nu} = e^{-2\varphi} g_{\mu\nu} - 2 \sinh(2\varphi) U_\mu U_\nu, \quad (5)$$

where  $\varphi$  is a scalar field and  $U_\mu$  is a normalized vector field with  $g^{\mu\nu} U_\mu U_\nu = -1$ . Both fields are dynamical. Therefore, the TeVeS action is the sum of three terms: the standard Einstein-Hilbert action, the action term for the scalar field

$$S_\varphi = -\frac{1}{2k^2\ell^2 G} \int \mathcal{F}(k\ell^2 h^{\alpha\beta} \varphi_{,\alpha} \varphi_{,\beta}) (-g)^{1/2} d^4x, \quad (6)$$

where  $\mathcal{F}$  is an arbitrary positive function,  $k$  is a dimensionless coupling constant,  $\ell$  a constant scale length, and  $h^{\alpha\beta} = g^{\alpha\beta} - g^{\alpha\mu} g^{\beta\nu} U_\mu U_\nu$ , and the action term for the vector field

$$S_U = -\frac{1}{32\pi G} \int [K g^{\alpha\beta} g^{\mu\nu} U_{[\alpha,\mu]} U_{[\beta,\nu]} + \bar{K} (g^{\alpha\beta} U_{\alpha;\beta})^2 - 2\lambda (g^{\mu\nu} U_\mu U_\nu + 1)] (-g)^{1/2} d^4x, \quad (7)$$

where the square brackets indicate antisymmetrisation,  $K$  and  $\bar{K}$  are dimensionless coupling constants and  $\lambda$  is a Lagrange multiplier to guarantee the normalization of  $U_\mu$ .

TeVeS violates the local Lorentz invariance, because at each point in spacetime there is a preferred frame in which the time coordinate aligns with  $U_\mu$ . The violation of Lorentz invariance derives from the invalidity of the Strong Equivalence Principle anticipated in Sect. 2. Clearly this violation has to be smaller than current experimental bounds.

In the limit  $K, \bar{K}, 1/\ell \rightarrow 0$ , with  $k \sim \ell^{-2/3}$ , for quasi-static systems and homogeneous cosmology, TeVeS corresponds to GR. To recover MOND in the non-relativistic ultra-weak field limit (equation 1), we need to choose the function  $\mathcal{F}$ . The arbitrariness of the function  $\mathcal{F}$  makes TeVeS a family of models, rather than a single model. The function  $\mathcal{F}$  proposed by Bekenstein [13] yields the MOND acceleration scale

$$a_0 = \frac{\sqrt{3k}}{4\pi\ell}. \quad (8)$$

As we have just mentioned, we recover GR in the limit  $K, \bar{K} \rightarrow 0$ , whereas to recover Newtonian gravity in the weak field limit  $\ell \rightarrow \infty$  suffices. Therefore, in principle, TeVeS and GR might differ in the strong field regime [79].

In the weak field limit, and quasi-static system, the geodesic metric becomes

$$\tilde{g}_{\mu\nu} dx^\mu dx^\nu = -(1 + 2\Phi) dt^2 + (1 + 2\Psi) \delta_{ij} dx^i dx^j. \quad (9)$$

This metric is formally identical to GR, where  $\Phi = -\Psi = \phi_N$  and  $\phi_N$  is the Newtonian gravitational potential. In this limit, in TeVeS we also have  $\Phi = -\Psi$ , but  $\Phi = \Xi \phi_N + \varphi$ , where  $\Xi = (1 - K/2)^{-1} e^{-2\varphi_c} \sim 1$ , with  $\varphi_c$  the asymptotic boundary

---

<sup>4</sup> In this section, we use units where the speed of light  $c = 1$ .

value of  $\phi$ . It appears clear that the scalar field  $\phi$  plays the role that DM plays in the standard model.

Equation (9) enables us to derive the gravitational lensing equations in TeVeS. In Sect. 3 we have seen that MOND excellently describes the dynamics of galaxies but requires some additional DM on the scales of clusters. One can thus anticipate that the description of gravitational lensing with TeVeS fits the observations on galaxy scales without the need of any matter in addition to the observed baryonic matter, but it does not do as well on cluster scales.

In fact, the TeVeS gravitational lensing equations applied to the strong lensing regime on galaxy scales reproduce the lensing morphology with the observed baryonic matter alone, both in simple spherically symmetric models of the lens [32, 152] and in models departing from spherical symmetry [131]. These analyses self-consistently include TeVeS cosmology, because of the cosmological distances of the lenses: it is easy to get erroneous results if one uses hybrid theories like MOND combined with GR rather than TeVeS itself [53]. In addition, claimed inadequacies of TeVeS [86] may be easily healed by assuming different, but still perfectly reasonable, mass models for the lens [33]. When analysed properly, to date no lensing system on galaxy scale appears to be problematic, including lensed quasars [31, 30, 33]. TeVeS even returns a measure of the Hubble constant consistent with other independent estimates when its time-delay formula is applied to lensed variable quasars [141]. Nevertheless, the debate on the adequacy of TeVeS to describe lensing data on galaxy scales is still open and lively [52].

Lensing of clusters returns the mass discrepancy that one encounters with the analysis of galaxy kinematics or X-ray emission. Because of the complexity of the covariant theories of MOND, the lensing analysis usually assumes spherical symmetry and quasi-stationarity. Relatively relaxed clusters, where these assumptions are substantially valid, show the expected mass discrepancies [138, 108]. DM halos are required, and it was suggested that DM in MOND could be made of neutrinos [125]. However, the neutrino phase-space density must be smaller than the Tremaine-Gunn limit we describe below in Sect. 5.1. The combination of strong and weak gravitational lensing data shows that the DM central density of MONDian clusters is larger than the Tremaine-Gunn limit for neutrino masses smaller than 7 eV [108]; this mass exceeds by more than a factor of three the experimental upper limits on the neutrino mass and this result suggests that neutrinos are inadequate MONDian DM particles.

The Bullet cluster is usually held as the definitive proof of the existence of collisionless DM [35]. Unfortunately, it is a difficult lens to model in MOND covariant theories because of its large departure from the assumptions mentioned above of spherical symmetry and quasi-stationarity. Figure 5 shows the results of one of the first TeVeS analyses of the Bullet cluster [11]: the convergence map is computed by assuming four spherically symmetric mass distributions at the location of the two galaxy distributions and the two X-ray emitting gas clouds. The model agrees with observations if the galaxies are embedded in additional halos of collisionless matter. Angus et al. [11] concluded that massive neutrinos with 2 eV mass accounting for two thirds of the total mass of the system is sufficient to reproduce the lens-

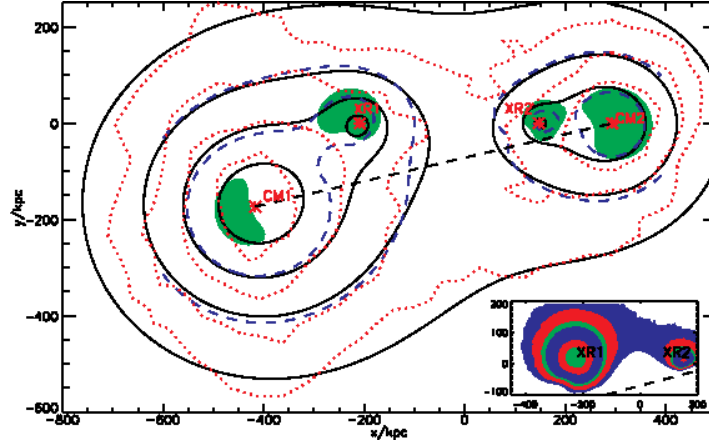


**Fig. 5** The solid black contours show the MOND-ian convergence map of the Bullet cluster [11]. The dotted red contours show the GR convergence map [35]. The contour levels are  $[0.37, 0.30, 0.23, 0.16]$ . The red stars indicate the centres of the four potentials used. The blue dashed lines show the contours of surface density  $[4.8, 7.2] \times 10^2 M_{\odot} pc^{-2}$  for the MOND standard  $\mu$  function. In the green shaded region the matter density is larger than  $1.8 \times 10^{-3} M_{\odot} pc^{-3}$  and indicate the clustering of 2 eV neutrinos. *Inset:* The surface density of the gas in the Bullet cluster predicted by a collisionless matter subtraction method for the standard  $\mu$ -function described in [11]. The contour levels are  $[30, 50, 80, 100, 200, 300] M_{\odot} pc^{-2}$ . The origin is  $[06^h 58^m 24^s .38, -55^{\circ} 56' .32]$ . Reproduced from [11].

ing signal. This amount of additional mass agrees with the results of the dynamical analysis of other clusters in MOND reviewed in Sect. 3.5, but, it became clear later [7, 108], as we mention earlier, that the conclusion about the 2 eV mass neutrinos is erroneous. The non-linearity of TeVeS does not seem to be conducive to removing the demand for DM in the Bullet cluster [50]. On the other hand, the effect of the external gravitational field, that plays a role in the internal dynamics of dSphs, or the non-trivial features that the additional TeVeS fields can induce in the lensing phenomena remain to be investigated [51].

## 5 MOND and Sterile Neutrinos

MOND assumes the existence of an acceleration scale below which an ultra-weak field limit of the theory of gravity sets in. From this very simple *ansatz*, MOND describes with impressive success the dynamics of galaxies and smaller systems. On the scale of galaxy clusters, MOND partly fails (Figure 2) and the observed kinematics require either a new gravity law or the existence of some baryonic or non-baryonic DM. This failure is bound to be shared by any covariant theory, like TeVeS, that is conceived to yield MOND in the ultra-weak field limit.

For most cosmologists, this failure implies the end of MOND as a successful description of the Universe. However, the DM paradigm currently is far from being satisfactory on galactic scales [75]. Therefore, if we are interested in finding a theory that describes the Universe with the minimum number of assumptions, we have to consider the possibility that MOND can indeed be a valid description of the observed phenomenology and look for possible solutions of its shortcomings on larger scales.

Similarly to the standard model, a natural solution is the introduction of some form of DM. However, we might have an advantage over the standard model. In a MONDian model with DM, DM has to be hot enough to freely stream out of galactic systems, to preserve the excellent description of the galactic dynamics without DM, but cold enough to cluster on the scale of galaxy clusters. Unlike the hypothetical cold DM particles, we know that an elementary particle that can play the role of hot DM does exist: the neutrino.

The properties of neutrinos are currently constrained by various experimental results. In 1979, Tremaine and Gunn [143], by considering the maximum mass density that DM halos made of light leptons can reach, set a lower limit of  $\sim 1$  MeV to the mass of the light leptons that can make the DM halos of galaxies and clusters of galaxies. Below, we briefly review this argument for its relevance to the subsequent discussion.

### 5.1 The Tremaine-Gunn Limit

Neutrinos are collisionless particles, and, according to Liouville's theorem, the phase-space fluid they form is incompressible. In practice, if neutrinos make the DM in self-gravitating systems, like galaxy clusters, this theorem sets an upper limit to the observable coarse-grained phase space density.

If self-gravitating systems form by violent relaxation, the neutrino coarse-grained phase-space density is  $f(\mathbf{x}, \mathbf{v}) = f(\varepsilon) = f_0 \{1 + \exp[\beta(\varepsilon - \chi)]\}^{-1}$ , where  $\varepsilon = \mathbf{v}^2/2 + \phi(\mathbf{x})$ ,  $\phi(\mathbf{x})$  is the gravitational potential,  $\sigma^2(\mathbf{x}) = 1/\beta$  is the 1D velocity dispersion,  $\chi$  is the neutrino chemical potential, and  $f_0 = g_v m_v^4 h^{-3}$  is the mass phase-space density of an occupied microcell;  $g_v = 2$  is the number of degrees of freedom, which includes the anti-particles,  $m_v$  is the neutrino mass, and  $h$  the Planck constant.

For a non-degenerate neutrino fluid, we have  $f(\varepsilon) \ll f_0$  which implies  $\beta(\phi - \chi) \gg 0$  and the phase-space density must be smaller than the Maxwell-Boltzmann distribution  $f_{\text{MB}}(\varepsilon) = f_0 \exp[-\mathbf{v}^2/2\sigma^2(\mathbf{x})]$ . Therefore, for the neutrino mass density  $\rho_v(\mathbf{x})$ , we must have  $\rho_v(\mathbf{x}) \leq 4\pi \int_0^{+\infty} v^2 f_{\text{MB}}(\varepsilon) dv = f_0 [2\pi\sigma^2(\mathbf{x})]^{3/2}$ . This relation implies that  $\max\{f\} = f_0 \geq \rho_v(\mathbf{x}) [2\pi\sigma^2(\mathbf{x})]^{-3/2}$ . However, clusters form from the relic neutrino background that has the Fermi distribution  $f(p) = f_0 [1 + \exp(pc/k_B T)]^{-1}$ , with  $p$  the momentum and  $T = 1.95$  K the neutrino temperature today. The initial maximum coarse-grained phase-space density is therefore  $\max\{f\} = f(p=0) = f_0/2$ . According to Liouville's theorem, this upper limit cannot increase, and we must thus have

$$\rho_v(\mathbf{x}) \leq \frac{f_0}{2} [2\pi\sigma^2(\mathbf{x})]^{3/2}. \quad (10)$$

For a fully degenerate gas, all the microcells with  $v < v_{\text{lim}}$  are occupied and  $f(\varepsilon) = f_0$ , whereas all the microcells with  $v > v_{\text{lim}}$  are empty and  $f(\varepsilon) = 0$ . Therefore, in this case, the neutrino mass density is  $\rho_v(\mathbf{x}) \leq f_0 4\pi \int_0^{v_{\text{lim}}} v^2 dv = f_0 4\pi v_{\text{lim}}^3/3$ . By considering only bound states with  $\varepsilon = \mathbf{v}^2/2 + \phi(\mathbf{x}) \leq 0$ , we have  $\mathbf{v}^2 \leq 2|\phi| \equiv v_{\text{lim}}^2$ , and thus  $\rho_v(\mathbf{x}) \leq f_0 4\pi |2\phi|^{3/2}/3$ . By assuming  $3\sigma^2 = -\phi$ , we obtain  $\rho_v(\mathbf{x}) \leq f_0 [2\pi\sigma^2(\mathbf{x})]^{3/2} 4(3/\pi)^{1/2}$ , which implies that the maximum phase-space density is  $\max\{f\} = f_0 \geq \rho_v(\mathbf{x}) [2\pi\sigma^2(\mathbf{x})]^{-3/2} (3/\pi)^{-1/2}/4$ . However, applying Liouville's theorem again with the initial maximum phase-space density  $f_0/2$ , we obtain the more stringent upper limit to the neutrino density

$$\rho_v(\mathbf{x}) \leq \frac{f_0}{2} [2\pi\sigma^2(\mathbf{x})]^{3/2} 4 \left(\frac{3}{\pi}\right)^{1/2}, \quad (11)$$

which is  $4(3/\pi)^{1/2} \approx 3.91$  times larger than the density upper limit obtained in the non-degenerate case [78, 144]. Therefore the non-degenerate case yields the most restrictive upper limit and is usually called the Tremaine-Gunn limit.

We can write this limit in astrophysical interesting units as

$$\rho_v \leq 2.16 \times 10^2 \left(\frac{m_v}{\text{eV}}\right)^4 \left(\frac{\sigma}{c}\right)^3 \frac{M_\odot}{\text{pc}^3} \quad (12)$$

or, by considering the relation  $k_B T / \mu m_p = \sigma^2$  between temperature and velocity dispersion, with  $m_p$  the proton mass and  $\mu = 0.6$  the mean atomic weight for a fully ionized gas of solar abundance,

$$\rho_v \leq 4.64 \times 10^{-7} \left(\frac{m_v}{\text{eV}}\right)^4 \left(\frac{k_B T}{\text{keV}}\right)^{3/2} \frac{M_\odot}{\text{pc}^3}. \quad (13)$$

## 5.2 The Role of an 11 eV Sterile Neutrino

The mass contribution of the three ordinary (active) neutrinos of the standard model,  $\nu_e$ ,  $\nu_\mu$ , and  $\nu_\tau$ , could, in principle, solve the mass discrepancy in MONDian galaxy clusters. At the end of the nineties, laboratory experiments yielded an upper bound limit to the mass of ordinary neutrinos of 2.2 eV [61]. Therefore, neutrinos with mass 2 eV were proposed as DM in MONDian models [125]. However, when their contributions to the properties of astrophysical sources, namely galaxy clusters, CMB and massive galaxies, are analyzed in details, the ordinary neutrinos with mass smaller than this limit are shown to be inadequate.

Sanders [125] and Pointecouteau and Silk [118] pointed out the relevance of the Tremaine-Gunn limit in galaxy clusters in MOND. An extensive analysis of 26 X-ray emitting groups and clusters of galaxies [7] considered neutrinos with

the maximum mass allowed by the current upper limits. These neutrinos have a Tremaine-Gunn limit that is at least a factor of two smaller than the DM density within 100 kpc that is required to describe the thermal properties of the intra-cluster medium in MOND. Therefore, either neutrinos are more massive, that is excluded by laboratory measurements, or they are not the major contribution to the MOND DM in clusters.

The three species of ordinary neutrinos with mass in the range  $1 - 2$  eV also are problematic when we attempt to reproduce the CMB power spectrum. These neutrinos suppress the third peak by  $\sim 25\%$  when compared to observations, because of their free-streaming imposed by the Tremaine-Gunn limit [88]. We can obtain a CMB power spectrum consistent with observations with these neutrinos in TeVeS if we substantially increase the MOND acceleration scale  $a_0$  at the time of recombination [133]. However, this redshift dependence of  $a_0$  remains unproved observationally.

Finally, the amplitude of the weak lensing signal around luminous galaxies ( $L > 10^{11} L_\odot$ ), extracted from the Red-Sequence Cluster Survey and the Sloan Digital Sky Survey, suggests mass-to-light ratios larger than  $\sim 10 M_\odot/L_\odot$  in the MOND framework [140]. It thus follows that DM is also required on the scale of massive galaxies. This DM cannot be made of ordinary neutrinos that are not massive enough to cluster on these small scales.

The inadequacies of ordinary neutrinos with any mass smaller than the current upper limits to properly describe this astrophysical phenomenology forces us to conclude that ordinary neutrinos as the MONDian DM are ruled out.

MOND can still be viable if we resort to hot DM made of sterile neutrinos. Sterile neutrinos do not have standard weak interactions and are right-handed, unlike the three ordinary neutrinos, and are motivated by a number of anomalies observed in neutrino experiments (see [1] for an extensive review). For example, the existence of one sterile neutrino in addition to the three ordinary neutrinos can elegantly explain the disappearance of electron neutrinos from the low energy beam measured in short-baseline neutrino oscillation experiments [59, 60, 77, 109].

If sterile neutrinos are more massive than ordinary neutrinos, they can have larger Tremaine-Gunn limits, and thus eventually solve the problems we mentioned above. The analysis of the MiniBooNE experiment data does indeed favour a sterile neutrino mass in the  $4 - 18$  eV range [58]. This mass range is inconsistent with cosmological constraints in the  $\Lambda$ CDM framework that would require the mass to be smaller than 1 eV (see, e.g., [60] and references therein). However, this mass limit derives from the enhanced gravity on galactic scales that is required by the standard model but not by MOND. Therefore, in MOND, the  $4 - 18$  eV mass range might be perfectly reasonable.

It is actually quite impressive that a universe with baryonic matter and one massive sterile neutrino alone reproduces very well the observed CMB power spectrum if the sterile neutrino mass is  $m_{\nu_s} = 11$  eV [3], a value that is fully consistent with the mass range inferred from the MiniBooNE data. In addition, the sterile neutrino mass must be within  $\sim 10\%$  of the 11 eV value if we wish to keep the good match with the observed CMB power spectrum. This strong constraint is mostly due to the

fact that, in this case, the contribution of the sterile neutrinos to the density of the Universe is  $\Omega_{\nu_s} h^2 = 0.117$ . This value is comparable to the contribution of CDM in the standard model that we know to describe the CMB power spectrum very well. It is important to remind that this analysis assumes that the sterile neutrinos are fully thermalised at the time of decoupling; more massive sterile neutrinos are possible but they must not be fully thermalised [24].

Figure 6 shows that the CMB power spectra of the standard  $\Lambda$ CDM model and of a model with baryonic matter and an 11 eV sterile neutrino are indistinguishable. Note that at the time of recombination, the average gravitational field is strong enough that the Universe is not in the MOND regime, with  $a_0$  kept constant to the present day value; therefore, the CMB power spectrum can be estimated with the standard theory of gravity. It is only at later times that the existence of such a massive neutrino would be problematic for the formation of structure in the standard model.

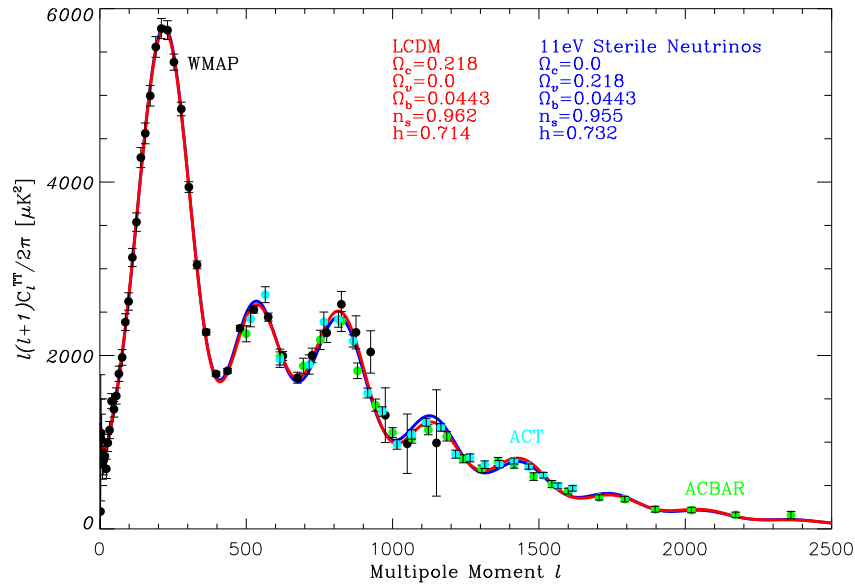


**Fig. 6** CMB angular power spectra for a cosmological model with baryons and an 11 eV sterile neutrinos (blue line), and for the  $\Lambda$ CDM model (red line). The points show data from WMAP year 7 (black), ACT (turquoise) and ACBAR (green). Reproduced from [5].

On the contrary, in MOND this massive sterile neutrino would be adequate to solve the mass discrepancy on the cluster scale. In fact, the study of the hydrostatic equilibrium configuration of 30 groups and clusters of galaxies, including the two clumps forming the Bullet cluster system, by the analysis of the profiles of the galaxy velocity dispersion and hot gas temperature, shows that the mass density pro-



file of DM made of 11 eV neutrinos always reaches the Tremaine-Gunn limit in the cluster center [8]. Some of the dynamical mass must be provided, as expected, by the central galaxies, but the required amount implies a mass-to-light ratio of  $1.2M_{\odot}/L_{\odot}$  in the K band, in agreement with stellar population synthesis models. An 11 eV sterile neutrino is also consistent with the straight arc, originated by a strong lensing effect, observed in the cluster A2390 [49].

It is remarkable that the 11 eV sterile neutrino required to match the CMB power spectrum also solves the completely independent problem of the mass discrepancy of MONDian clusters without requiring any additional free parameter or adjustment of the model. It is also intriguing that the Tremaine-Gunn limit is always reached in the cluster centers, implying that the dynamical properties of clusters are uniquely set by the mass of the sterile neutrino. This relation is completely unknown to the standard DM paradigm, where the mass of the cold DM particle does not have any role in the dynamical properties of clusters.

It remains to be seen whether gravitational instability in a universe filled of baryonic matter and one species of sterile neutrino with 11 eV mass can form the observed cosmic structure at the correct pace, although we remind that the ability to explain the cluster mass discrepancy does not directly imply that MOND combined with 11 eV sterile neutrinos can form clusters in a cosmological context.

The investigation of structure formation in this model requires an efficient  $N$ -body code and proper cosmological initial conditions. Previous  $N$ -body simulations of MOND do not consider the presence of any non-baryonic DM and the adopted initial conditions might not be consistent for a universe filled with baryons alone. These previous  $N$ -body simulations show an overproduction of cosmic structure in a baryon-only MONDian universe, in obvious disagreement with observations [110, 83].

A first attempt of  $N$ -body simulation of structure formation in a MONDian universe with baryons and an 11 eV sterile neutrino has been performed with a particle-mesh cosmological  $N$ -body code that solves the modified Poisson equation of the quasi-linear formulation of MOND (QUMOND) and with initial conditions appropriate to DM made of 11 eV neutrinos [5]. The simulation evolved a box of  $512h^{-1}$  Mpc on a side with  $256^3$  particles from redshift  $z = 250$  to the present time.

This MONDian hot DM model does indeed produce galaxy clusters with the correct order of magnitude of the abundance of observed X-ray clusters, unlike hot DM models with standard gravity that have structure formation suppressed on small scales [29]. However the model overproduces the X-ray luminous clusters by a factor of three and underproduces the low luminosity clusters with  $T < 4.5$  keV by at least a factor of ten. Nevertheless the density profiles of the simulated clusters are compatible with the observed profiles of MONDian clusters. In addition, the frequency of relative velocities larger than  $3000 \text{ km s}^{-1}$  of cluster pairs is large enough to make likely, unlike the standard model [80], the occurrence of systems like the Bullet cluster.

Overall the results of this simulation are somewhat unsatisfactory. However, the simulation has the very poor mass and length resolutions  $\sim 10^{12}M_{\odot}$  and  $\sim 2$  Mpc, respectively; therefore clustering on small scales is artificially suppressed and this



can partly explain the severe underestimate of the abundance of low-luminous X-ray clusters. The underproduction of low massive clusters could also be quelled by swapping the 11 eV sterile neutrino for a more massive, up to 1 keV, sterile neutrinos, because the free-streaming scale decreases with increasing mass of the DM particle. As we mentioned above, however, these higher mass sterile neutrinos would not be fully thermalised prior to decoupling. The overproduction of massive clusters and supercluster size objects actually is a problem that MOND has with any mass of sterile neutrino or any other DM particle.

In addition, the expansion of the Universe is assumed to coincide with the standard Friedmann-Robertson-Walker model with a cosmological constant. It is doubtful that a self-consistent relativistic version of MOND will be close enough to the standard model to be consistent with current observational limits on the expansion history of the Universe, but discrepant enough to yield the correct structure formation rate. Structure formation is affected by the acceleration scale  $a_0$  which sets the enhancement of the intensity of the gravitational field compared to standard gravity. Currently, we do not have any observational constraints on the redshift dependence of  $a_0$ , but if  $a_0$  is lower at higher redshift, the overproduction of cosmic structure could be suppressed and the abundance of massive clusters could become consistent with observations. However, this feature would suppress galaxy formation and is therefore not ideal.

Clearly, the phenomenological formulation of MOND is not conceived to yield a self-consistent cosmological model, and a covariant model including MOND needs to be implemented to test its predictions of structure formation robustly. For example, the linear perturbation theory of the density field in TeVeS has already been outlined [132], but the non-linear evolution of cosmic structure, with or without a non-baryonic DM component, still needs to be investigated.

## 6 Conclusion

MOND is based on the *ansatz* that Newtonian dynamics is modified when the gravitational field determined by the distribution of baryonic matter drops below the acceleration  $a_0 \sim 10^{-10} \text{ m s}^{-2}$  [94]. The observational evidence for the existence of this acceleration scale has been rapidly accumulating over the last decade. The success of MOND at describing the dynamics of self-gravitating systems up to the scale of galaxies with fewer parameters than the standard DM paradigm is undeniable: in the standard model, the additional gravitational force that is required by the observed kinematics is supplied by the presence of proper amounts of DM, but this solution requires, unlike MOND, a number of fine tunings and coincidences to explain the existence of the acceleration scale that emerges at different length scales. MOND provides a far simpler explanation of these observations.

In addition, on the scale of galaxies, MOND has an impressive predictive power that is alien to the DM paradigm. Numerous observations predicted by MOND were confirmed years later. One of the most striking was that, if interpreted in Newtonian

dynamics, the kinematics of LSB galaxies imply that DM dominates the dynamics of these systems more than in any other system in the Universe [95].

However, on the scale of galaxy clusters, MOND still requires some form of DM, although not as much as in the DM paradigm [7]. Reproducing the power spectrum of the CMB beyond the second peak also requires some non-baryonic DM [88].

In principle, neutrinos might represent a possible candidate for this non-baryonic DM. However, current upper limits on the ordinary neutrino mass show that they would not be massive enough to condense in the core of clusters and preserve the height of the third peak of the CMB power spectrum, as required by observations.

A viable alternative candidate is a sterile neutrino. This particle seems to be required to interpret a number of anomalous results from neutrino experiments [1]. A sterile neutrino with mass in the range  $11\text{ eV} - 1\text{ keV}$  would ensure DM hot enough to stream out of galaxies but cold enough to cluster on the scale of massive galaxies and beyond. It is thus in principle capable of explaining the phenomenology of astrophysical systems preserving the success of MOND on small scales and, in principle, the success of the standard model on large scales [3]. Such a model, where we have a modification of gravity and an exotic DM particle, might be more attractive than the current standard  $\Lambda$ CDM model, because of its elegance on the scale of galaxies, the physical motivation of the existence of its DM particle from experiments on Earth and, eventually, the fact that it requires fewer free parameters than  $\Lambda$ CDM. However, it remains to be investigated whether this model can reproduce the full phenomenology of the large-scale structure formation and evolution.

Moreover, this model rests on MOND, that is still a classical theory, not a covariant theory. The parent covariant theory that gives MOND in the proper limit is still unknown. Many possibilities have been proposed, but none of them appears yet to be fully convincing.

The exciting conclusion is that, whatever model is going to be correct, the existence of the acceleration scale, that the data on galaxy scales indicates with astonishing regularity, has to be explained naturally by the correct model, unless a number of surprising coincidences happen to fool us.

**Acknowledgements** We thank Benoit Famaey and Stacy McGaugh for useful suggestions and for providing us with Figures 1, 2, 3, and 4. We thank Ana Laura Serra for a careful reading of the manuscript and Luisa Ostorero for enlightening and encouraging discussions. AD gratefully acknowledges partial support from INFN grant PD51 and PRIN-MIUR-2008 grant 2008NR3EBK\_003 “Matter-antimatter asymmetry, dark matter and dark energy in the LHC era”. GWA is supported by the Claude Leon Foundation and a University Research Committee Fellowship from the University of Cape Town. This research has made use of NASA’s Astrophysics Data System.

## References

1. Abazajian, K. N., Acero, M. A., Agarwalla, S. K., et al. 2012, arXiv:1204.5379
2. Angus, G. W. 2008, MNRAS, 387, 1481
3. Angus, G. W. 2009, MNRAS, 394, 527

4. Angus, G. W., Diaferio, A. 2009, MNRAS, 396, 887
5. Angus, G. W., Diaferio, A. 2011, MNRAS, 417, 941
6. Angus, G. W., McGaugh, S. S. 2008, MNRAS, 383, 417
7. Angus, G. W., Famaey, B., Buote, D. A. 2008, MNRAS, 387, 1470
8. Angus, G. W., Famaey, B., Diaferio, A. 2010, MNRAS, 402, 39
9. Angus, G. W., Famaey, B., Zhao, H. S. 2006, MNRAS, 371, 138
10. Angus, G. W., van der Heyden, K., Diaferio, A. 2012, A&A, in press
11. Angus, G. W., Shan, H. Y., Zhao, H. S., Famaey, B. 2007, ApJL, 654, L13
12. Angus, G. W., Diaferio, A., Kroupa, P. 2011, MNRAS, 416, 1401
13. Bekenstein, J. D. 2004, Phys. Rev. D, 70, 083509
14. Bekenstein, J. D. 2012, arXiv:1201.2759
15. Bekenstein, J., Milgrom, M. 1984, ApJ, 286, 7
16. Bell, E. F., McIntosh, D. H., Katz, N., Weinberg, M. D. 2003, ApJS, 149, 289
17. Bernal, T., Capozziello, S., Cristofano, G., de Laurentis, M. 2011, Modern Physics Letters A, 26, 2677
18. Bertone, G., Hooper, D., Silk, J. 2005, Phys. Rep., 405, 279
19. Bianchi, E., Rovelli, C. 2010, arXiv:1002.3966
20. Bienaymé, O., Famaey, B., Wu, X., Zhao, H. S., Aubert, D. 2009, A&A, 500, 801
21. Bigiel, F., Leroy, A., Walter, F., et al. 2010, AJ, 140, 1194
22. Bournaud, F. 2010, Advances in Astronomy, 1 (arXiv:0907.3831)
23. Bovy, J., Dvorkin, C. 2012, arXiv:1205.2083
24. Boyanovsky, D. 2008, Phys. Rev. D, 78, 103505
25. Boylan-Kolchin, M., Bullock, J. S., Kaplinghat, M. 2012, MNRAS, 422, 1203
26. Bradač, M., Allen, S. W., Treu, T., et al. 2008, ApJ, 687, 959
27. Bryan, G.L., Norman, M.L., 1998, ApJ, 495, 80
28. Cardone, V. F., Angus, G., Diaferio, A., Tortora, C., Molinaro, R. 2011, MNRAS, 412, 2617
29. Cen, R., Ostriker, J. P. 1992, ApJ, 399, 331
30. Chen, D.-M. 2008, JCAP, 1, 6
31. Chen, D.-M., Zhao, H. 2006, ApJL, 650, L9
32. Chiu, M.-C., Ko, C.-M., Tian, Y. 2006, ApJ, 636, 565
33. Chiu, M.-C., Ko, C.-M., Tian, Y., Zhao, H. 2011, Phys. Rev. D, 83, 063523
34. Ciotti, L., Binney, J. 2004, MNRAS, 351, 285
35. Clowe, D., Bradač, M., Gonzalez, A. H., et al. 2006, ApJL, 648, L109
36. Cole, D. R., Dehnen, W., Read, J. I., Wilkinson, M. I. 2012, arXiv:1205.6327
37. de Bernardis, P., Ade, P. A. R., Bock, J. J., et al. 2002, ApJ, 564, 559
38. Desmond, H. 2012, arXiv:1204.1497
39. Diaferio, A. 2008, The evidence for unusual gravity from the large-scale structure of the Universe, in From the Vacuum to the Universe, Proceedings of the 1<sup>st</sup> AFI Symposium (Innsbruck, Austria, October 2007), edited by S.D. Bass, F. Schallhart and B. Tasser, Innsbruck University Press, p. 71-85 (arXiv:0802.2532)
40. Diaferio, A. 1999, MNRAS, 309, 610
41. Duc, P.-A. 2012, arXiv:1205.2297
42. Dutton, A. A. 2012, arXiv:1206.1855
43. Eckmiller, H. J., Hudson, D. S., Reiprich, T. H. 2011, A&A, 535, A105
44. Einasto, J., Kaasik, A., Saar, E. 1974, Nature, 250, 309
45. Faber, S. M., Jackson, R. E. 1976, ApJ, 204, 668
46. Famaey, B., Bruneton, J.-P., Zhao, H. 2007, MNRAS, 377, L79
47. Famaey, B., Binney, J. 2005, MNRAS, 363, 603
48. Famaey, B., McGaugh, S. 2011, arXiv:1112.3960
49. Feix, M., Zhao, H., Fedeli, C., Pestaña, J. L. G., Hoekstra, H. 2010, Phys. Rev. D, 82, 124003
50. Feix, M., Fedeli, C., Bartelmann, M. 2008, A&A, 480, 313
51. Ferreira, P. G., Starkman, G. D. 2009, Science, 326, 812
52. Ferreras, I., Mavromatos, N., Sakellariadou, M., Furqaan Yusaf, M. 2012, arXiv:1205.4880
53. Ferreras, I., Sakellariadou, M., Yusaf, M. F. 2008, Phys. Rev. Lett., 100, 031302
54. Fraternali, F., Sancisi, R., Kamphuis, P. 2011, A&A, 531, A64

55. Gentile, G., Famaey, B., Angus, G., Kroupa, P. 2010, *A&A*, 509, A97
56. Gentile, G., Famaey, B., Combes, F., et al. 2007, *A&A*, 472, L25
57. Gerbal, D., Durret, F., Lachieze-Rey, M., Lima-Neto, G. 1992, *A&A*, 262, 395
58. Giunti, C., Laveder, M. 2008, *Phys. Rev. D*, 77, 093002
59. Giunti, C., Laveder, M. 2011, *Phys. Rev. D*, 83, 053006
60. Giunti, C., Laveder, M. 2011, *Phys. Rev. D*, 84, 093006
61. Groom, D. E. 2000, *European Physical Journal C*, 15, 358
62. Guo, Q., White, S., Boylan-Kolchin, M., et al. 2011, *MNRAS*, 413, 101
63. Halle, A., Zhao, H., Li, B. 2008, *ApJS*, 177, 1
64. Hensler, G. 2012, *arXiv:1205.1243*
65. Humphrey, P. J., Buote, D. A., O’Sullivan, E., Ponman, T. J. 2012, *arXiv:1204.3095*
66. Ibata, R., Sollima, A., Nipoti, C., et al. 2011, *ApJ*, 738, 186
67. Jee, M. J., Mahdavi, A., Hoekstra, H., et al. 2012, *ApJ*, 747, 96
68. Kashlinsky, A., Atrio-Barandela, F., Ebeling, H. 2012, *arXiv:1202.0717*
69. Kirkman, D., Tytler, D., Suzuki, N., O’Meara, J. M., Lubin, D. 2003, *ApJS*, 149, 1
70. Klimentowski, J., Łokas, E. L., Knebe, A., et al. 2010, *MNRAS*, 402, 1899
71. Komatsu, E., Smith, K. M., Dunkley, J., et al. 2011, *ApJS*, 192, 18
72. Kosowsky, A. 2010, *Advances in Astronomy*, 2010, 4
73. Kravtsov, A. 2010, *Advances in Astronomy*, 2010, 8
74. Kravtsov, A. V., Gnedin, O. Y. 2005, *ApJ*, 623, 650
75. Kroupa, P. 2012, *arXiv:1204.2546*
76. Kroupa, P., Famaey, B., de Boer, K. S., et al. 2010, *A&A*, 523, A32
77. Kuflik, E., McDermott, S. D., Zurek, K. M. 2012, *arXiv:1205.1791*
78. Kull, A., Treumann, R. A., Böhringer, H. 1996, *ApJL*, 466, L1
79. Lasky, P. D., Sotani, H., Giannios, D. 2008, *Phys. Rev. D*, 78, 104019
80. Lee, J., Komatsu, E. 2010, *ApJ*, 718, 60
81. Leroy, A. K., Walter, F., Brinks, E., et al. 2008, *AJ*, 136, 2782
82. Li, Y.-S., Helmi, A. 2008, *MNRAS*, 385, 1365
83. Llinares, C., Knebe, A., Zhao, H. 2008, *MNRAS*, 391, 1778
84. Mahdavi, A., Hoekstra, H., Babul, A., Balam, D. D., Capak, P. L. 2007, *ApJ*, 668, 806
85. Mastropietro, C., Burkert, A. 2008, *MNRAS*, 389, 967
86. Mavromatos, N. E., Sakellariadou, M., Yusaf, M. F. 2009, *Phys. Rev. D*, 79, 081301
87. McGaugh, S. S. 2004, *ApJ*, 609, 652
88. McGaugh, S. S. 2004, *ApJ*, 611, 26
89. McGaugh, S. S. 2005, *ApJ*, 632, 859
90. McGaugh, S. S. 2008, *IAU Symposium*, 244, 136
91. McGaugh, S. S. 2008, *ApJ*, 683, 137
92. McGaugh, S. S., de Blok, W. J. G. 1998, *ApJ*, 499, 66
93. McGaugh, S. S., Wolf, J. 2010, *ApJ*, 722, 248
94. Milgrom, M. 1983, *ApJ*, 270, 365
95. Milgrom, M. 1983, *ApJ*, 270, 371
96. Milgrom, M. 1983, *ApJ*, 270, 384
97. Milgrom, M. 1984, *ApJ*, 287, 571
98. Milgrom, M. 1995, *ApJ*, 455, 439
99. Milgrom, M. 1998, *ApJL*, 496, L89
100. Milgrom, M. 2002, *ApJL*, 577, L75
101. Milgrom, M. 2007, *ApJL*, 667, L45
102. Milgrom, M. 2008, *New Astron. Rev.*, 51, 906
103. Milgrom, M. 2010, *MNRAS*, 403, 886
104. Milgrom, M. 2012, *arXiv:1205.1308*
105. Milgrom, M., Sanders, R. H. 2003, *ApJL*, 599, L25
106. Mirabel, I. F., Dottori, H., Lutz, D. 1992, *A&A*, 256, L19
107. Moore, B., Ghigna, S., Governato, F., et al. 1999, *ApJL*, 524, L19
108. Natarajan, P., Zhao, H. 2008, *MNRAS*, 389, 250
109. Nelson, A. E. 2011, *Phys. Rev. D*, 84, 053001

110. Nusser, A. 2002, MNRAS, 331, 909
111. Oort, J. H. 1932, Bulletin of the Astronomical Institutes of the Netherlands, 6, 249
112. Ostriker, J. P., Peebles, P. J. E. 1973, ApJ, 186, 467
113. O'Sullivan, E., Forbes, D. A., Ponman, T. J. 2001, MNRAS, 328, 461
114. Pawlowski, M. S., Kroupa, P., de Boer, K. S. 2011, A&A, 532, A118
115. Pawlowski, M. S., Kroupa, P., Angus, G., et al. 2012, arXiv:1204.6039
116. Pireaux, S. 2004, Classical and Quantum Gravity, 21, 1897
117. Pireaux, S. 2004, Classical and Quantum Gravity, 21, 4317
118. Pointecouteau, E., Silk, J. 2005, MNRAS, 364, 654
119. Reiprich, T. H. 2001, Ph.D. Thesis, Ludwig-Maximilians-Universität
120. Roberts, M. S., Rots, A. H. 1973, A&A, 26, 483
121. Romanowsky, A. J., et al. 2003, Science, 301, 1696
122. Sánchez-Salcedo, F. J., Reyes-Iturbide, J., & Hernandez, X. 2006, MNRAS, 370, 1829
123. Sanders, R. H. 1997, ApJ, 480, 492
124. Sanders, R. H. 2000, MNRAS, 313, 767
125. Sanders, R. H. 2003, MNRAS, 342, 901
126. Sanders, R. H. 2012, MNRAS, 419, L6
127. Sanders, R. H. 2012, MNRAS, 422, L21
128. Schubert, Y., Richtler, T., Hilker, M., Salinas, R., Dirsch, B., Larsen, S. S. arXiv:1205.2093
129. Serra, A. L., Angus, G. W., Diaferio, A. 2010, A&A, 524, A16
130. Serra, A. L., Diaferio, A., Murante, G., Borgani, S. 2011, MNRAS, 412, 800
131. Shan, H. Y., Feix, M., Famaey, B., Zhao, H. 2008, MNRAS, 387, 1303
132. Skordis, C. 2006, Phys. Rev. D, 74, 103513
133. Skordis, C., Mota, D. F., Ferreira, P. G., Boehm, C. 2006, Physical Review Letters, 96, 011301
134. Simon, J. D., Geha, M. 2007, ApJ, 670, 313
135. Smoot, G. F., Bennett, C. L., Kogut, A., et al. 1992, ApJL, 396, L1
136. Spergel, D. N., Bean, R., Doré, O., et al. 2007, ApJS, 170, 377
137. Steinmetz, M., Navarro, J. F. 1999, ApJ, 513, 555
138. Takahashi, R., Chiba, T. 2007, ApJ, 671, 45
139. The, L. S., White, S. D. M. 1988, AJ, 95, 1642
140. Tian, L., Hoekstra, H., Zhao, H. 2009, MNRAS, 393, 885
141. Tian, Y., Ko, C.-M., Chiu, M.-C. 2012, arXiv:1204.6359
142. Tiret, O., Combes, F., Angus, G. W., Famaey, B., Zhao, H. S. 2007, A&A, 476, L1
143. Tremaine, S., Gunn, J. E. 1979, Physical Review Letters, 42, 407
144. Treumann, R. A., Kull, A., Böhringer, H. 2000, New Journal of Physics, 2, 11
145. Tully, R. B., Fisher, J. R. 1977, A&A, 54, 661
146. van der Kruit, P. C., Freeman, K. C. 2011, ARA&A, 49, 301
147. Vikhlinin, A., Kravtsov, A., Forman, W., et al. 2006, ApJ, 640, 691
148. Walker, M. G. 2012, arXiv:1205.0311
149. Walker, M. G., Mateo, M., Olszewski, E. W., et al. 2007, ApJL, 667, L53
150. Wyder, T. K., Martin, D. C., Barlow, T. A., et al. 2009, ApJ, 696, 1834
151. Zhang, Y.-Y., Andernach, H., Caretta, C. A., et al. 2011, A&A, 526, A105
152. Zhao, H., Bacon, D. J., Taylor, A. N., Horne, K. 2006, MNRAS, 368, 171
153. Zwicky, F. 1933, Helv. Phys. Acta, 6, 110